Repeatability of adaptation in sunflowers: genomic regions harbouring inversions also drive adaptation in species lacking an inversion

Shagheyegh Soudi[1+], Mojtaba Jahani[1,2+], Marco Todesco[2,3,4], Gregory L. Owens[5], Natalia Bercovich[2], Loren H. Rieseberg[2], Sam Yeaman[1,*]

+Joint first-authors

Author affiliations:

1. Department of Biological Sciences, University of Calgary, 2500 University Drive NW, Calgary, Canada, T2N 1N4
2. Department of Botany, University of British Columbia, 6270 University Blvd, Vancouver, Canada, V6T 1Z4
3. Michael Smith Laboratories, University of British Columbia, 6270 University Blvd, Vancouver, Canada, V6T 1Z4
4. Irving K. Barber Faculty of Science, University of British Columbia Okanagan, 3187 University Way, Kelowna, Canada, V1V 1V7
5. Department of Biology, University of Victoria, 3800 Finnerty Rd, Victoria, Canada, V8P 5C2

*corresponding author: Sam Yeaman, samuel.yeaman@ucalgary.ca

Abstract

Local adaptation commonly involves alleles of large effect, which experience fitness advantages when in positive linkage disequilibrium (LD). Because segregating inversions suppress recombination and facilitate the maintenance of LD between locally adapted loci, they are also commonly found to be associated with adaptive divergence. However, it is unclear what fraction of an adaptive response can be attributed to inversions and alleles of large effect, and whether the loci within an inversion could still drive adaptation in the absence of its recombination-suppressing effect. Here, we use genome-wide association studies to explore patterns of local adaptation in three species of sunflower: *Helianthus annuus*, *H. argophyllus*, and *H. petiolaris*, which each harbour a large number of species-specific inversions. We find evidence of significant genome-wide repeatability in signatures of association to phenotypes and environments, which are particularly enriched within regions of the genome harbouring an inversion in one species. This shows that while inversions may facilitate local adaptation, at least some of the loci involved can still make substantial contributions without the benefit of recombination suppression. While a large number of genomic regions show evidence of repeated adaptation, most of the strongest signatures of association still tend to be species-specific, indicating substantial genotypic redundancy for local adaptation in these species.

Introduction

The genetic basis of local adaptation is sometimes highly repeatable, with examples of large effect genes driving responses in multiple species, such as *FT* affecting flowering time in numerous plants (Izawa 2007; Auge et al. 2019) or *Mc1r* driving colour polymorphisms in vertebrates (Manceau et al. 2010; Rosenblum et al. 2014). Local adaptation can also be repeated for polygenic traits, with significant patterns of similar association found across many loci for comparisons of conifers (Yeaman et al. 2016), maize and its wild relative teosinte (Tittes et al. 2021; Wang et al. 2021), and *Brassicaceae* (Bohutínská et al. 2021), to name a few. While we have a growing number of examples of repeatability in the basis of adaptation, it is also interesting to know if species use different genes to adapt to the same selection pressure. Genotypic redundancy – the potential for many genotypes to yield a given phenotype -- is one critical factor affecting the repeatability of adaptation, as high redundancy would be expected to result in lower repeatability (Yeaman et al. 2018). Another critical factor affecting repeatability

is shared standing variation, whether present due to introgression or incomplete lineage sorting. In either case, variants shared among lineages are much more likely to contribute to a repeated response than new mutations (MacPherson and Nuismer 2018; Ralph and Coop 2015). Consistent with this, Bohutínská and colleagues (2021) found that repeatability was negatively related to phylogenetic distance. While we are now accumulating more studies about the repeatability of adaptation, we still have very few examples and much remains unknown about the relative importance of these factors (Yeaman 2022).

Inversions have been implicated in local adaptation in many species (Wellenreuther and Bernatchez 2018), likely due to their effect to suppress recombination between any causal loci within their bounds (Rieseberg 2001; Noor et al. 2001; Kirkpatrick and Barton 2006). Despite mounting evidence of their importance in adaptation, it is unclear how inversions may covary with repeatability of adaptation among species. If most alleles have small effects relative to migration rate and can only contribute to local adaptation via the benefit of the recombination-suppressing effect of an inversion, then we would expect little repeatability at the site of an inversion – other species lacking the inversion would not tend to use that same region for adaptation. On the other hand, if some loci are particularly important for local adaptation and regularly yield mutations of large effect, with these patterns being conserved among species, repeatability within regions harbouring inversions may be substantial.

Here, we explore the repeatability of local adaptation in three species of sunflowers, *Helianthus annuus*, *Helianthus argophyllus* and *Helianthus petiolaris* (Figure 1), which harbour large regions of suppressed recombination ("haploblocks"), most of which are inversions, and are often associated with adaptive traits (Todesco et al. 2020). *Helianthus annuus*, the common sunflower, is the closest wild relative of cultivated sunflower, which was domesticated from it around 4,000 years ago (Blackman et al. 2011). Populations of *H. annuus* are distributed throughout the central and western USA and generally found on mesic soils, but can grow in a variety of disturbed or extreme habitats, such as semi-desertic or frequently flooded areas, as well as salt marshes. *Helianthus petiolaris*, the prairie sunflower, prefers sandier soils, and ecotypes of this species are adapted to sand sheets and sand dunes (Ostevik et al. 2016). Here we include samples from two subspecies: *H. petiolaris ssp. petiolaris*, which is commonly found in

86 the southern Great Plains, and *H. petiolaris ssp. fallax*, which is limited to more arid regions in
87 Colorado, Utah, New Mexico and Arizona (Heiser et al. 1969). *Helianthus petiolaris* and *H.*
88 *annuus* have broad and overlapping distributions throughout the central and western United
89 States and appear to have adapted to similar changes in temperature, moisture and photoperiod
90 regimes. There is also evidence indicating *H. annuus* and *H. petiolaris* have likely been
91 exchanging genes during much of their history of divergence (Strasburg and Rieseberg 2008),
92 although partially isolated by strong pre- and post-zygotic barriers (Sambatti et al. 2012). The
93 third species, *Helianthus argophyllus*, the silverleaf sunflower, is found exclusively in the
94 southeast coast of Texas and includes both an early flowering ecotype on the coastal barrier
95 islands and a late flowering ecotype inland (Moyers and Rieseberg 2016; Todesco et al. 2020).
96 *H. argophyllus* is thought to have undergone cycles of sympatry and allopatry with *H.*
97 *annuus* and *H. petiolaris* over time, but currently only overlaps with *H. annuus,* with thus
98 overlap likely being a recent event (Heiser, 1951).
99
100 Using broad sampling across the ranges of these species (Figure 1) and sequencing data
101 first published by Todesco et al. (2020), we study the genomic basis of local adaptation by
102 conducting genome-wide scans for associations with climatic and soil environmental variables
103 and phenotypes measured in a common garden. An inherent problem in studying the basis of
104 local adaptation is accounting for the covariance between genome-wide population genetic
105 structure and environment. When the selection pressure driving local adaptation tends to parallel
106 a main axis of demographic expansion or isolation by distance, neutral alleles will have spatial
107 patterns resembling those of causal alleles. Methods that do not correct for population structure
108 have large numbers of false positives because allele frequencies at neutral loci tend to correlate
109 with the environment more than expected by chance (Lotterhos and Whitlock 2014). By contrast,
110 methods that use structure correction tend to suffer from false negatives because the causal loci
111 have similar patterns of allele frequency variation as the genomic background, and so their
112 statistical signatures are decreased (DeRaad et al. 2021; Booker et al. 2023b). When a non-
113 corrected approach is applied to multiple species, the false positive problem can be mitigated
114 when testing for loci that contribute to repeated adaptation, as the same gene should not tend to
115 be a false positive in multiple species more often than expected by chance (Yeaman et al. 2016).
116 Here we use a conventional GWAS approach with structure correction to study the basis of

117 phenotypes, which vary both within and among populations, and use an uncorrected approach to
118 test association to environment, which only varies among populations (as all individuals within
119 the same population have the same value of environmental variable). For the environmental
120 association portions of the study, we also explore the effect of structure correction in some
121 analyses, to contrast the false negative vs. false positive problem inherent in each approach. We
122 apply these approaches individually to *H. annuus*, *H. argophyllus*, and the two *H. petiolaris*
123 subspecies, and make pairwise and higher-order comparisons among combinations of these four
124 lineages to study repeatability.
125
126 Our overall aim is to characterize the extent of repeatability of local adaptation for different traits
127 and environments, and explore the importance of inversions and other factors that may drive
128 differences in repeatability. This analysis builds upon the work of Todesco et al. (2020), which
129 focused on the evolution of haplobocks within each species, but did not systematically study
130 patterns of repeatability in signatures of association among species. We begin by using the
131 strength of correlations between environment and phenotypes measured in a common garden to
132 identify which environmental variables are likely driving local adaptation within each species,
133 and use an index to quantify the relative similarity in these patterns among pairs of species. We
134 then conduct Genome-Wide Association tests to identify regions most strongly associated with
135 phenotypes and environments within each species. To assess the similarity in these association
136 statistics among species, we use methods similar to Yeaman et al. (2016) to identify regions of
137 the genome that exhibit greater similarity in signatures of association among pairs of lineages
138 than expected by chance, and explore how the number and total size of these regions covaries
139 with the index of similarity in environmental importance. We also explore whether these regions
140 of repeated association tend to covary with patterns of shared standing variation and test if they
141 are enriched within previously identified haploblocks, to explore the role of inversions in
142 adaptation. We then identify candidate genes that show particularly strong signatures of repeated
143 association across multiple lineages. Finally, based on the number of signatures of association
144 that are shared vs. non-shared among lineages, we estimate the number of regions genome-wide
145 that could potentially contribute to local adaptation for each variable and phenotype, which is
146 related to the genotypic redundancy. Taken together, our results show that local adaptation in
147 sunflowers tends to involve both strong repeatability at a small number of genes, often associated

with inversions, coupled with high redundancy and non-repeated responses across a much larger number of loci.

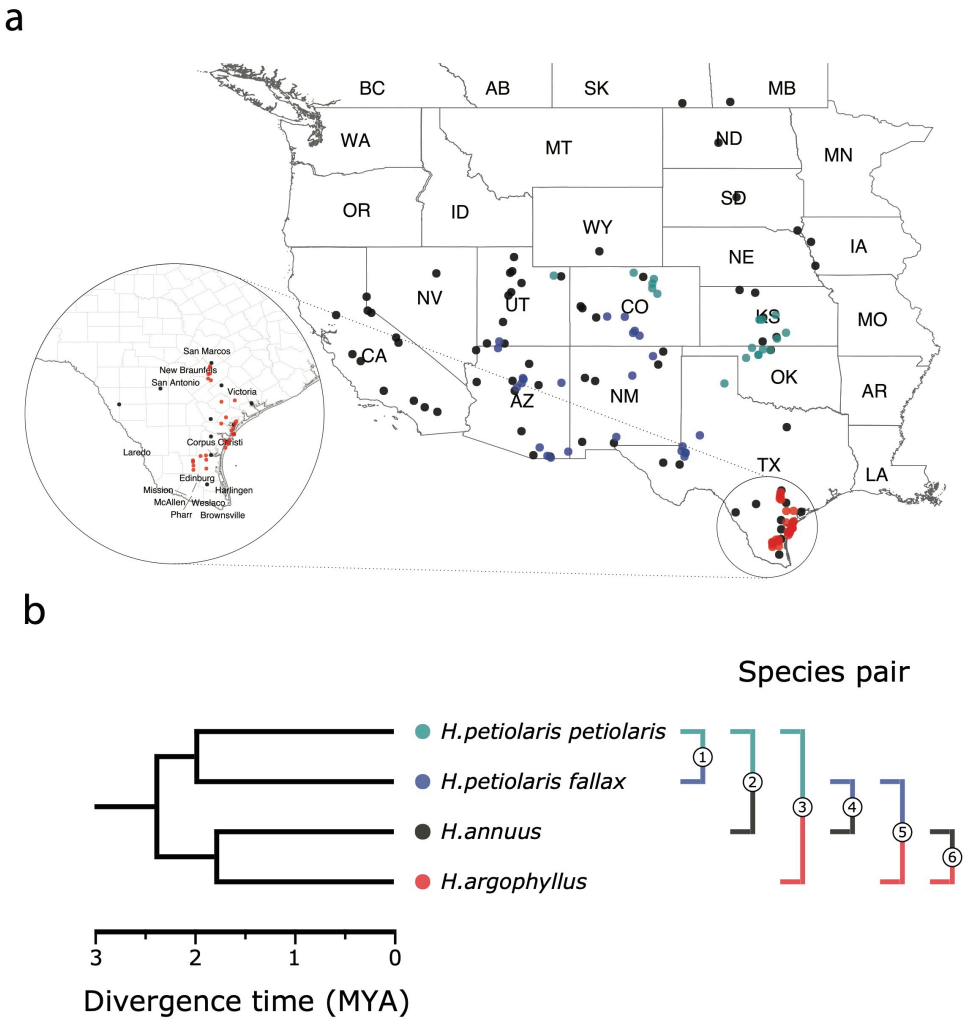

Figure 1. Sampling sites and phylogenetic relationship among surveyed species. (a) Sampling locations of wild sunflower populations studied in the present study, and (b) phylogenetic relationship of the four (sub-)species. Numbered brackets represent the six pairwise comparisons performed in this study.

Results

Local adaptation at the phenotypic level. The four taxa vary considerably in the breadth of environmental variation spanned by their respective ranges, with *H. annuus* spanning the widest niche and *H. argophyllus* spanning the narrowest (Figure 2A). We observe strong correlations for many combinations of phenotypes and environmental variables (Figure S1), suggesting that local adaptation is quite pronounced for some traits. To quantify the similarity in patterns of local adaptation among pairs of species, for each environmental variable we calculate an index we refer to as the Similarity in Phenotype-Environment Correlation (SIPEC), which is maximized when both species have strong correlations with the environmental variable across many phenotypes (see Methods). To prevent heavily weighting the contribution of multiple highly correlated phenotypes, we fit a principal components analysis to the phenotypes and used the resulting axes to calculate SIPEC. We find the largest values of SIPEC for temperature variables and the smallest values for soil types, and generally find higher values for comparisons between the *petiolaris* subspecies (Figure S2).

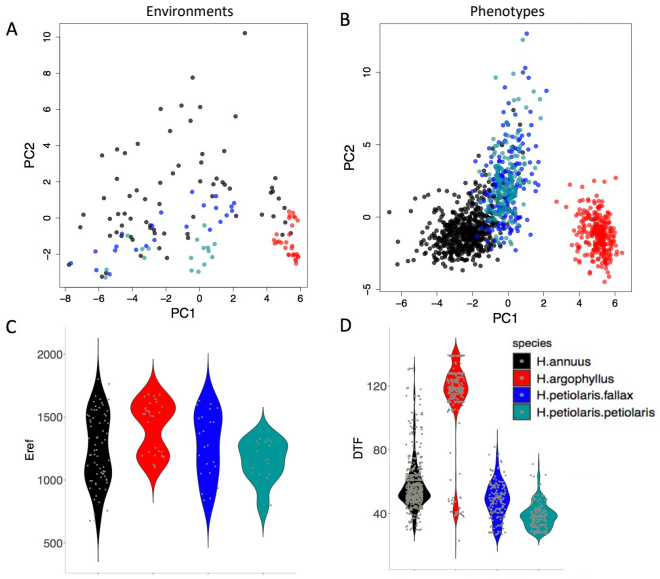

Figure 2. The range of environmental and phenotypic variation in the studied species.

Variation in environment (a) and phenotype (b) for the studied species, along the two largest axes of a Principle component analysis (PCA). Violin plots show two examples of variation in environment (Hargreaves reference evapotranspiration index; Eref) and phenotype (Days to Flower; DTF) within and among the taxa (c,d).

Genome-wide analysis of repeated local adaptation. To search for regions of the genome driving repeated adaptation in multiple taxa, we first identified windows of the genome within each species that showed strong signatures of association to either phenotype (GWAS) or environment (GEA), referred to as "top candidate" windows. To identify Windows of Repeated Association (WRAs) between pairs of species, we then assessed whether top candidate windows identified in one focal taxon also tended to be enriched for strong signatures of association to the same environment or phenotype in each of the other taxa (using the null-W test, which tends to be more sensitive than just finding the overlap between the top candidate windows; See Methods). As recombination rate can affect the sensitivity of these kinds of window-based genome scans (Booker et al. 2020), the identification of WRAs was conducted after binning windows by recombination rate, although in many cases we did not observe substantial differences in the null distributions among these bins (*e.g.*, Figure S3). This analysis revealed many windows with signatures of repeated association, with the strongest repeated signature found for Number of Frost-Free Days (NFFD; Figure 3A; S4), but also showed that many of the windows with the strongest association in one species did not have strong signatures in other species (Figure 3B).

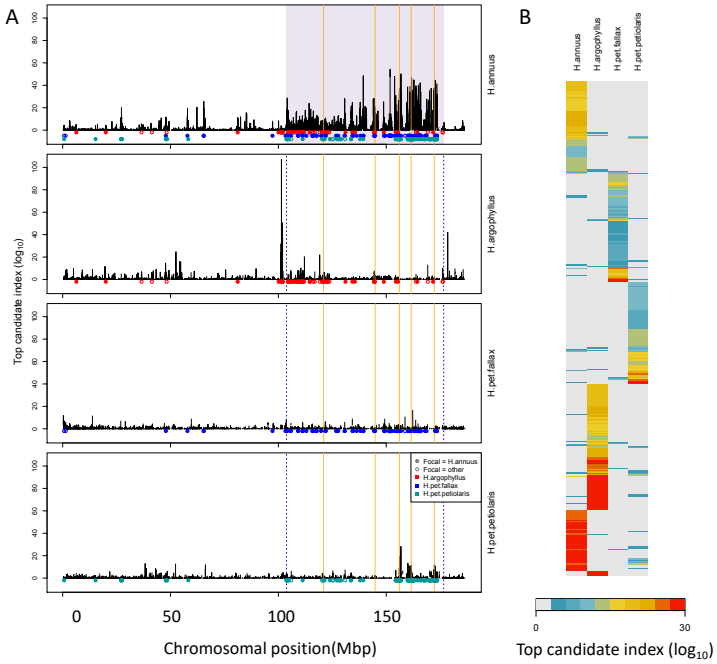

Figure 3. Signatures of association for Number of Frost-Free Days (NFFD) in the four taxa on chromosome 15 (A) and genome-wide (B). Panel A shows Windows of Repeated Association (WRAs; coloured bars) for comparisons between the focal species, *H. annuus*, and each of the other 3 taxa, with the haploblocks in *H. annuus* shaded in violet and the regions with significant PicMin hits as vertical orange lines. Panel B shows the value of the top candidate index for each of the 1000 windows with the strongest signatures of association in at least one species (~top 2% of genome-wide windows). Rows are ordered using hierarchical clustering to group windows with similar patterns across multiple species, illustrating the extent of overlap/non-overlap in the windows with strongest signatures in each species (*i.e.* position in the figure does not reflect chromosomal position).

Under the null hypothesis that all regions of the genome evolve neutrally due to drift and independently in each species, ~5% of the top candidate windows identified in one species would be expected to fall into the tail of the null distribution of another species (i.e. be classified as WRAs). While we find significantly more WRAs than the 5% expected by chance, ranging from 6.3% to 44.1% (mean = 14.5%; Figure S4), multiple factors can violate the assumptions of this test and increase the proportion of windows classified as WRAs. Most importantly, similarity in signatures of association can be driven by shared ancestral variation or ongoing

224 introgression, and this must always be considered as an alternative explanation. It is clear that
225 most regions of the genome harbour some shared standing variation between all 6 pairwise
226 comparisons of the taxa, whether due to segregating ancestral variation or introgression, based
227 on an index quantifying the proportion of shared to non-shared SNPs in each window (Figure
228 S5). However, we do not find consistent differences in the amount of shared standing variation
229 within windows when comparing WRAs with the rest of the genome (Figure S5). Thus, while
230 introgression may make subtle contributions to WRAs, a lack of increased shared standing
231 variation in the significant windows suggests that it is not a primary driver of these patterns.
232 A second source of inflation in the number of WRAs is due to hitchhiking: if a given
233 locus is a true positive driving adaptation, LD with other windows in tight physical linkage will
234 result in spurious correlations causing them to also be classified as WRAs increasing the
235 genome-wide proportion above 5%, and this effect will be particularly exaggerated in
236 haploblocks. To control for this, we binned neighbouring WRAs together that exhibited high LD
237 (>95th percentile) over short spans of the genome (<1 cM) in either species, yielding regions we
238 refer to as Clusters of Repeated Association (CRAs). While this clustering method should
239 provide a partial control for the effect of hitchhiking, we note that the number of CRAs cannot be
240 taken as a reliable estimate of the number of independent targets of natural selection. Instead, we
241 treat the number and size of these CRAs as proxies for the relative genome-wide similarity in
242 association between each pair of species, and conduct downstream analyses to test hypotheses
243 about the factors driving local adaptation.
244 CRAs varied in number and size across the 6 pairwise-species comparisons, with
245 particularly large CRAs identified at the sites of known haploblocks (Todesco et al. 2020). For
246 CRAs identified for phenotypic associations, their extent ranged from 168 clusters spanning
247 48,524,903 bp (covering only 1.6% of the genome) in *H.argophyllus-H.pet.petiolaris* to a
248 maximum of 1,667 clusters spanning 426,409,647 bp (14.2 % of the genome) in *H. pet.*
249 *petiolaris-H. pet. fallax* (Figure S6). CRAs identified for environmental variables tended to be
250 more numerous and cover a larger region of the genome, varying from 1154 clusters comprising
251 15% of the total genome for *H. argophyllus-H. pet. fallax* up to 2,260 distinct clusters covering
252 29% of the genome between *H. petiolaris* subspecies (Figure S7). The large extent of the
253 genome covered by CRAs is mainly driven by their occurrence within many different
254 haploblocks, which tend to be unique to each species and cover substantial portions their

genomes (Todesco et al. 2020). Genes within CRAs tend to be enriched for a large number of GO terms spanning many different categories (Figure S8, S9). When we use an approach that corrects for population structure in the genotype-environment association tests (Baypass), we find substantially reduced numbers of CRAs (Figure S10). This reduction is likely due to reduced power to detect true positive causal loci when population structure covaries with environment, as true positives do not "stand out" relative to the genomic background (Booker et al. 2023b). While single-species association tests without correction for population structure typically yield large numbers of false positives, the null-W test comparing association results across species accounts for the chance that the same region is a false positive in both species (Yeaman et al. 2016).

Repeated association in the genome reflects patterns at the phenotypic level. If natural selection is driving repeated patterns of local adaptation in the genomes of two species, we should see greater similarity for associations with environmental variables that are also strongly associated with phenotypic variation in both species. Consistent with this prediction, we found that environmental variables with a high SIPEC index (i.e. high correlation with phenotypes; Figure S2) also tended to have a larger number of CRAs in all comparisons (Figure 4), with higher repeatability at both the phenotype and genome level for temperature-related variables and much lower repeatability for soil-related variables. Unfortunately, given the non-independence of environmental variables it is not possible to conduct a formal significance test of these patterns. In all cases, the number of CRAs exhibited a weak negative relationship with the index of standing variation, with environmental variables that had the greatest number of CRAs having the lowest relative amounts of shared standing variation (Figure S11). This suggests that the observed similarity in patterns of association among species is not being strongly driven by incomplete lineage sorting or introgression, as we would expect a positive relationship between the index of shared standing variation and the number of CRAs. We found similar but weaker patterns in the association between SIPEC and size of CRAs (Figure S12), which may reflect comparatively greater contribution of haploblocks driving patterns with size rather than number (i.e. if a particularly large haploblock is a CRA, then that variable will have a particularly large value relative to its actual importance for local adaptation).

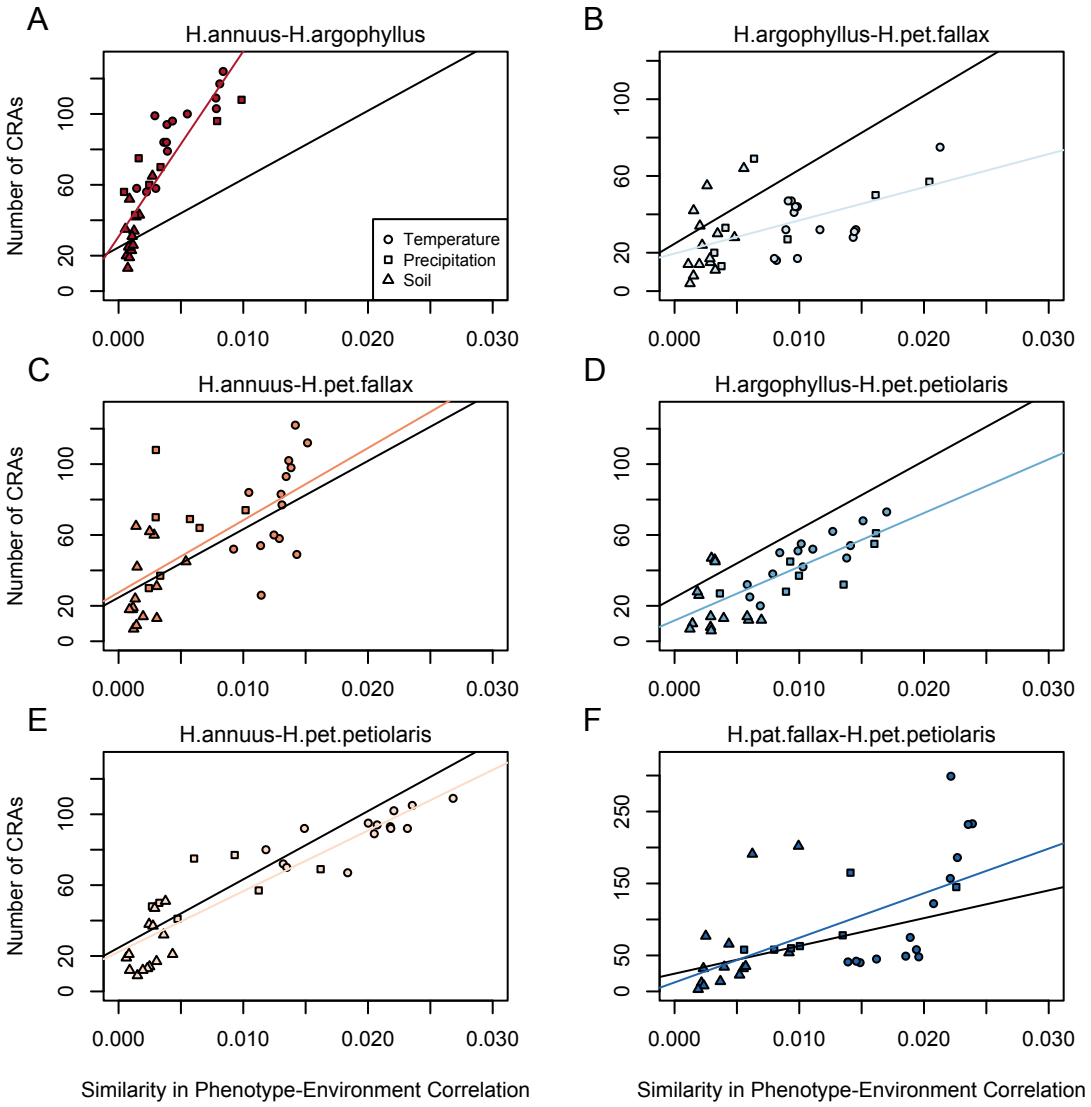

Figure 4. Relationship between mean Similarity in Phenotype-Environment Correlation (SIPEC) and number of Clusters of Repeated Association (CRAs). Each panel includes both a linear model fit to the data within the panel (coloured lines), and a linear model fit to all data simultaneously (black lines) for comparison.

Overlap of signatures of repeated association with low recombination haploblocks.

Inversions can facilitate local adaptation by suppressing recombination between locally adapted alleles within the inverted vs. ancestral haplotypes (Kirkpatrick and Barton 2006). If a given

species exhibits a signature of association to environment at a segregating inversion, it is interesting to test whether similar signatures of association are found in other species that lack a segregating inversion at the same region of the genome. This would suggest that particularly strong selection is acting on this region, as signatures of association can still evolve even without the recombination suppressing effect of the inversion. While not all of the low-recombination haploblocks identified by Todesco et al. (2020) have been validated as inversions, for simplicity we treat each haploblock as representative of a segregating inversion. The majority of these haploblocks are present as segregating variation in only one of the three species, but when they occur in *H. petiolaris*, they tend to be found as segregating variation within both subspecies. Thus, if we find significant enrichment of the regions of repeated association (WRAs and CRAs) within haploblocks, this suggests that both the species with a segregating inversion and the species lacking an inversion are using this region of the genome to drive local adaptation. As a first test of this relationship, we assessed two-way contingency tables for whether top candidate windows within a species were also significant windows of repeated association (WRA/non-WRA) and whether they fell within haploblocks (yes/no). This approach controls for the potential enrichment of top candidate windows within haploblocks relative to the rest of the genome and asks if the rate of WRAs within haploblocks is higher. For most phenotypes and environments, we found that the proportion of WRAs in haploblocks was much higher than for non-WRAs (Figure 5). Across all species comparisons and environmental/phenotypic variables, a total of 310 contrasts showed significant enrichment for WRAs in haploblocks, compared to only 23 contrasts showing a significantly higher proportion of non-WRAs in haploblocks. In *H. argophyllus*, while non-WRA top candidates tended to fall within haploblocks less commonly than in the other taxa, WRAs tended to be very strongly enriched within haploblocks (Figure 5B). As a follow-up, we also tested whether CRAs were enriched within haploblocks (without controlling for whether top candidate windows also tended to be enriched), also finding strongly significant enrichment of CRAs within haploblocks for many traits and environments (Figure S6C & D). Broad patterns revealed by these analyses are similar, as both show that regions with haploblocks tend to be enriched for signatures of association to environment in species lacking the haploblock. It is noteworthy that few significant signatures of enrichment in haploblocks were found for *H. petiolaris petiolaris* vs. *H. petiolaris fallax* (Figure S6C & D), perhaps

because extensive introgression across non-locally adapted regions of the genome obscures true signal.

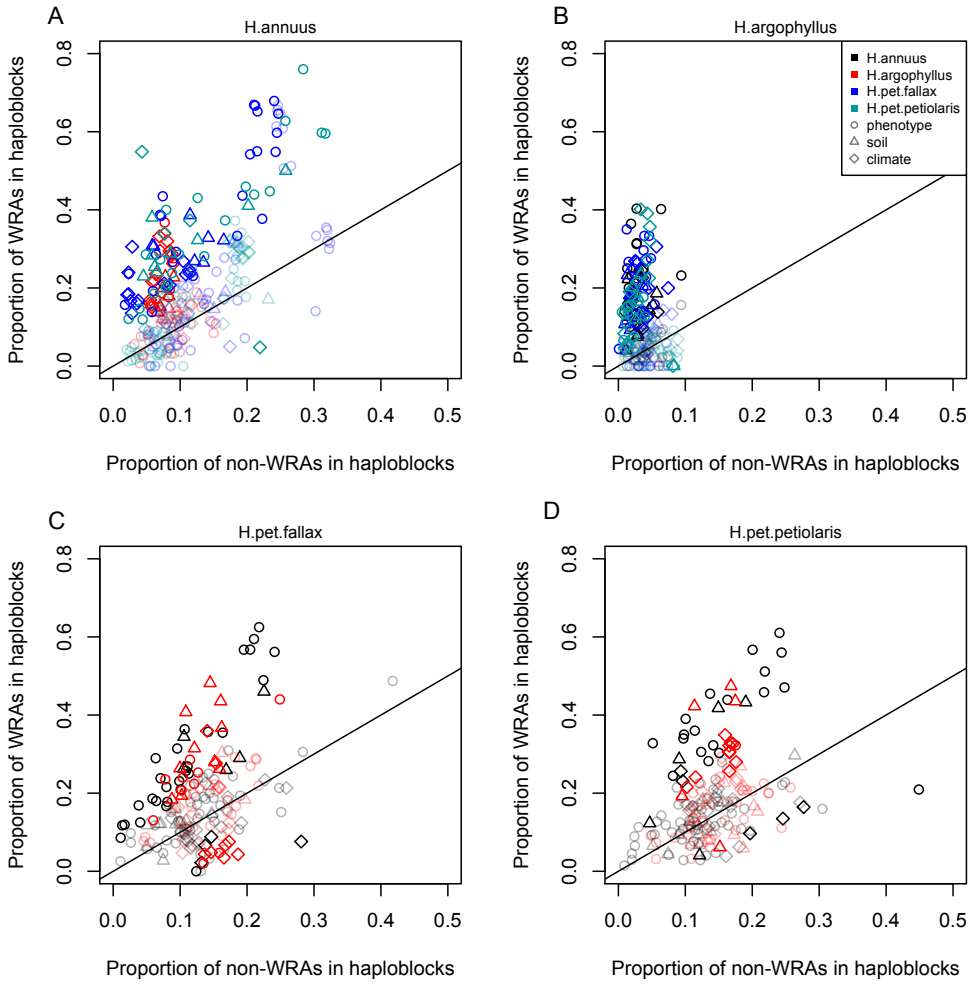

Figure 5. Enrichment of signatures of repeated association within genomic regions harbouring a haploblock in one of the two compared lineages. Each panel shows the proportion of top candidate genes that fall within haploblocks for windows with significant signatures of repeated association by the null-W test (WRAs) vs. those with non-significant signatures (non-WRAs). Comparisons of *H. petiolaris petiolaris* vs. *H. petiolaris fallax* are omitted as they share segregating haploblocks. Each point corresponds to the results for a single phenotype or environment, with dark shading used for cases where the deviation from random for the contingency table is significant by a permutation test ($p < 0.05$), and lighter shading indicating a non-significant result.

Multi-species signatures of repeated association. As a complement to the pair-wise analyses described above, we also conducted an analysis using PicMin, which simultaneously considers

346 any number of lineages to identify genes with particularly strong and repeated signatures of
347 association (Booker et al. 2023a). After clustering together windows < 1 Mbp apart, we found a
348 total of 145 regions that were significant for at least one variable or phenotype (at FDR < 0.1
349 applied within each variable). The largest number of significant regions for environment was
350 found with the Number of Frost-Free Days variable (20 with FDR < 0.1; 44 with FDR < 0.2) and
351 for phenotypes with Total Leaf Number, a measure of developmental timing of flowering (9
352 with FDR < 0.1; 19 with FDR < 0.2). Considering the 720 individual 5000 bp windows with
353 FDR < 0.2 for at least one variable, 387 are within 500 bp of a genic region, representing a 2.3x
354 enrichment relative to the rate for windows that were not significant hits using PicMin (23.3% of
355 other windows fall within 500 bp of a genic region; X^2 test $p < 10^{-15}$).
356

357

358 **Estimating the number of potentially adaptive loci.** Even for the environment with the highest
359 repeatability (Number of Frost-Free Days; NFFD), most of the strongest signals of association
360 are found in only one lineage (Figure 3B). Unfortunately, while the null-W test provides strong
361 support and controls false positives when identifying repeated association, regions of the genome
362 with strong associations in only a single species may include a large (and unknown) number of
363 false positives. Thus, while it is biologically interesting to know how much adaptation is non-
364 repeated among species, it is difficult to quantify with certainty (Booker et al. 2023a; Booker et
365 al. 2023b). Under the assumption that at least some of the non-repeated signatures of association
366 are true positives, this implies that there is considerable genotypic redundancy, with many
367 different ways for these species to adaptively respond to variation in the same environment. To
368 estimate the number of windows that could potentially contribute to local adaptation for each
369 variable (L_{eff}), we modified the method of Yeaman et al. (2018) to partially account for the effect
370 of linkage among nearby windows (see methods). This method assumes that the windows with
371 signatures of association in each species are a random draw from a larger number of potentially
372 contributing windows (L_{eff}), which can be inferred based on the ratio of shared vs. non-shared
373 windows with strong association signatures (see Methods). We find that estimates of L_{eff} tend to
374 be large, always well over 1000 windows regardless of the trait or environment (Figure S13A).
375 There are numerous sources of error that affect the estimation of L_{eff}, which will tend to be

overestimated due to linkage (Figure S13A) or when many signatures of association are false positives (see supplementary results), and will be underestimated when some repeatability is due to shared standing variation (Yeaman et al. 2018). Even after controls for linkage and assuming a high false positive rate of 80%, estimates of L_{eff} remain in the hundreds even for the variable with the lowest value of L_{eff} (Eref; Figure S13C, D).

Discussion

Despite its critical importance in shaping the architecture of adaptation, little is known about the extent of genotypic redundancy underlying different traits (Barghi et al. 2020; Láruson et al. 2020; Yeaman 2022). Here, we have shown evidence of significant repeatability in the basis of local adaptation (Figure 4, 5), but also an abundance of species-specific, non-repeated signatures (Figure 3; S13). In particular, we find that regions of the genome that harbour inversions in one species also tend to be strongly enriched for signatures of association in other species lacking the inversion (Figure 5). Taken together, this suggests that local adaptation in these species is highly flexible -- different species apparently use quite different sets of loci to adapt to the same environment -- yet still involves some component that has minimal redundancy, with inversions playing a particularly important role. Some of the "usual suspects" show up in the set of significantly repeated loci identified by PicMin: in addition to the homologs of the *FT* (*FLOWERING LOCUS T*) gene reported by (Todesco et al. 2020), we also found hits for several other genes involved in circadian regulation and flowering time, including *PRR3* (Para et al. 2007)), *TOE1* (Aukerman and Sakai 2003), and *PHYC* (Takano et al. 2005; Chen et al. 2014), which is known to regulate photoperiodic responses in Arabidopsis accessions (Balasubramanian et al. 2006). Other top hits included genes involved in plant development and auxin transport (*PIN3*; (Keuskamp et al. 2010), *ARF4* (Pekker et al. 2005), and *MN*; (Bhatia et al. 2016)), and plant immunity (*CRK13* (Acharya et al. 2007) and *PRR2* (Cheval et al. 2017))

404 The increased repeatability found in regions of the genome that harbour inversions in only
405 one species is particularly interesting. Inversions are commonly associated with local adaptation
406 (Wellenreuther and Bernatchez 2018), likely because they reduce the rate at which
407 recombination breaks up combinations of co-selected alleles (Kirkpatrick and Barton 2006),
408 which perhaps facilitates contributions by alleles that would be individually too weakly selected
409 to overcome swamping by migration (Bürger and Akerman 2011; Yeaman and Whitlock 2011;
410 Schaal et al. 2022). Evidence here suggests these regions still tend to contribute to adaptation in
411 the species lacking the recombination-suppressing effect of an inversion, consistent with a strong
412 effect of selection relative to migration on at least one locus in the region. Given that under this
413 model, inversions will be most likely to persist if they capture multiple locally adapted alleles,
414 the observation of enrichment of signatures of repeated adaptation within inversions could also
415 explain their long-term persistence. If there is variation across the genome in the density of loci
416 with the potential to be involved in local adaptation, then the evolution and maintenance of
417 locally adaptive inversions would be biased towards co-occuring with the loci most likely to be
418 involved in local adaptation. If the potential for local adaptation is conserved amongst species,
419 then these same regions are more likely to have high repeatability. In this way, repeatability in
420 inversion-containing regions may reflect the preferential retention of inversions, as well as the
421 retention of locally adaptive alleles. As an example, chromosome 15 harbours a large (72 Mbp)
422 haploblock in *H. annuus* that is strongly associated with NFFD (Number of Frost-Free Days),
423 and also shows some signatures of association in the other taxa, with particularly strong
424 signatures of association on either side of the haploblock in *H. argophyllus* (Figure 3A).
425 Interestingly, loci of repeated association identified by PicMin within this region include two
426 genes whose homologs are known to regulate responses to cold: *COLD-RESPONSIVE*
427 *PROTEIN KINASE 1*,*CRPK1* (Liu et al. 2017)) and *LATE ELONGATED HYPOCOTYL*, *LHY*
428 (Mizoguchi et al. 2002; Dong et al. 2011). While many studies have demonstrated the
429 importance of inversions for adaptation (Wellenreuther and Bernatchez 2018; Hager et al. 2022),
430 to our knowledge only one other study has documented the involvement of the same loci making
431 contributions in the absence of the recombination-suppressing effect of the inversion (Lee et al.
432 2017). This also highlights how comparative studies of a species lacking an inversion may help
433 identify which genes are driving adaptation in another species with an inversion, as segregating

434 inversions tend to have extensive LD that prevents identification of any potential targets of
435 natural selection within them.

436 While our results suggest a large number of loci can potentially contribute to adaptation,
437 implying high redundancy (Figure 3B; S13), there are several factors that complicate inference.
438 Separating the effects of drift and selection to detect signatures of local adaptation is notoriously
439 difficult, because population structure often covaries with features of the environment that drive
440 adaptation (Lotterhos and Whitlock 2014; Hoban et al. 2016; DeRaad et al. 2021). As found by
441 other analyses (Yeaman et al. 2016; DeRaad et al. 2021), when we use structure correction in our
442 genotype-environment association tests, we find many fewer signatures of repeated association
443 (Figure S6 vs. S10), likely due to the reduced power of Baypass to detect true positives when the
444 environment covaries with population structure (Booker et al. 2023b). Here, we have side-
445 stepped the issues involved in correction for population structure by instead relying on
446 comparisons among species to identify loci with associations more extreme than expected by
447 chance, using the null-W and PicMin tests. This assumes that most loci in the genome are not
448 involved in local adaptation, so that the relatively small proportion that are driving adaptation
449 can therefore be picked out due to their tendency to fall into the tail of the distribution of
450 association statistics. While this approach should be relatively robust for identifying loci with
451 repeated patterns of adaptation, there is no way to formally estimate significance of associations
452 found in only a single species, many of which may be false positives due to covariation of
453 population structure and environment. However, even if we assume that 80% of the observed
454 non-repeated loci are false positives, we still find that estimates of the effective number of loci
455 contributing to adaptation (L_{eff}) are in the hundreds (Figure S13C). As we are unable to detect
456 loci of small effect due to the limited power, our estimates of L_{eff} will also be biased downwards
457 by excluding these potentially important drivers. Finally, it is also difficult to exclude the
458 contribution of introgression or incomplete lineage sorting to the observed signatures repeated
459 association. If a locus tended to be highly introgressed between two species in a restricted region
460 of their range, it is possible it could also covary with environment and therefore result in a
461 signature of repeated association that would be mistakenly interpreted as adaptation. While it is
462 difficult to preclude this from our analysis, regions of the genome with signatures of repeated
463 association do not tend to have higher levels of shared standing variation than background

464 regions (Figure S5), suggesting this is not a broad explanation for our observations. If anything,
465 shared standing variation would be expected to increase repeatability of adaptation (MacPherson
466 and Nuismer 2017), adding further weight to the inference that there is high genotypic
467 redundancy in these species.

468 In general, we find that temperature is the strongest driver of repeated adaptation at both
469 the phenotypic and genomic levels. We quantified local adaptation at the phenotypic level using
470 correlations between traits measured in common gardens and the home environment of the
471 population they were sampled from. Across all phenotypes, these correlations tended to be
472 strongest and most similar among species for temperature variables, particularly in comparisons
473 among *H. annuus* and *H. petiolaris* subspecies (Figure S2). We see similar patterns of
474 repeatability reflected in the genome, where temperature variables also tend to have the greatest
475 repeatability (Figure 4). The similarity in these phenotypic and genomic signatures is consistent
476 with an effect of strong selection, as other artefactual or drift-based explanations for repeatability
477 would not be expected to reflect patterns found at the phenotypic level. It should be noted that
478 the reduced importance of soil variables in the SIPEC index might be partly driven by the fact
479 that all traits were measured on above-ground features, due to the difficulty of getting non-
480 disruptive phenotypic measurements for roots.

481 Taken together, these results suggest that some fraction of the genome contributes to adaptation
482 with low redundancy and high repeatability (which tend to be enriched within inversions), while
483 the remainder of the adaptive response is driven by loci with high redundancy and species-
484 specific contributions. Models in evolutionary genetics tend to focus on extremes: population
485 genetic approaches explore cases where strong selection deterministically drives a change in
486 allele frequency, whereas quantitative genetic approaches make the infinitesimal assumption that
487 phenotypic change can be realized through small frequency changes at many loci (Barton et al.
488 2017; Barghi et al. 2020; Yeaman 2022). Our results suggest that adaptation is a complex
489 process that does not map cleanly onto the assumptions of either approach, but that at least some
490 component of trait variation experiences sufficiently strong selection to overcome migration and
491 drift and behave in a way approximately consistent with population genetic models. Given the
492 difficulty of rigourously quantifying the contribution of alleles of small effect, it remains an open
493 question what proportion of adaptive response is governed by loci with dynamical behaviour that

494 follow the infinitesimal assumption. This could perhaps be quantified explicitly by decomposing
495 trait heritabilities as has been done for standing variation in humans (Visscher et al. 2017), but
496 this would require a considerable increase in sample size as methods such as GCTA (Yang et al.
497 2011) do not yield accurate estimates at the sample sizes used here.

498

499 **Materials and Methods**

500 **Data collection, common garden, and phenotyping.** Seed samples were collected from 151
501 wild sunflower populations covering most of their native distributions during the summer of
502 2015 (*H. annuus*: 61 populations for GWAS and 71 populations for GEA, *H. petiolaris fallax*: 23
503 populations, *H. petiolaris petiolaris:* 18 populations and *H. argophyllus*: 30 populations, Figure
504 1 and Supplementary Table 1). Seeds from ten additional populations of *H. annuus* for the GEA
505 analysis had been previously collected in the summer of 2011. Sample seeds were obtained from
506 randomly chosen mothers, and were first germinated in a greenhouse for two weeks, later moved
507 to an open-sided greenhouse for acclimation. Phenotypic data were collected throughout the
508 growing season, as detailed in Supplementary Table 1. Extensive records of developmental and
509 morphological traits throughout the growth of the plants including leaves, stem, and seeds which
510 were collected and digitally imaged to extract relevant phenotypic data.
511

512 **Similarity in Phenotype-Environment Correlation (SIPEC).** Locally adapted traits tend to
513 exhibit strong correlations between environment and common-garden phenotype, so
514 environments that are important to driving local adaptation should exhibit strong correlations
515 with many traits. As an index to represent the similarity among pairs of species in an
516 environment's average correlation across all measured phenotypes, we calculate SIPEC =
517 $\sum_i (|r_{i,1}| + |r_{i,2}|)|r_{i,1}||r_{i,2}|/n_p$ where $r_{i,1}$ and $r_{i,2}$ are the Pearson correlations between the
518 environment and the ith phenotype in the first and second species, respectively, and n_p is the
519 number of phenotypes. This SIPEC index is maximized when the correlation is large in both
520 species regardless of the direction, so it does not differentiate phenotypically convergent vs.
521 divergent patterns of local adaptation, and provides a means of estimating the relative importance
522 of an environment driving local adaptation across all measured phenotypes. To account for non-
523 independence among traits, for each pair of species we fit a PCA to all measured phenotypes and

524 use the Principal Components that collectively explain 95% of the variance, and calculate SIPEC
525 on the correlations of these variables with environment.

526

527 **Tests of SNP association with environment (GEA) and phenotype (GWAS).** A total of 39
528 environmental variables (21 climatic variables, 3 geographic variables, 15 soil variables
529 Supplementary Table 1) were used for the genotype-environment association analysis (GEA).
530 We refer to the climatic, soil and geographic variables collectively as the "environmental
531 variables", for simplicity. Soil data were collected by taking three to five soil samples collected
532 at each population from across the area in which seeds were collected and submitted to Midwest
533 Laboratories Inc. (Omaha, NE, USA) for analysis. Climate data for each population were
534 collected over a 30-year period (1961-1990) from geographic coordinates of the locations where
535 the samples were collected, using the software package Climate NA (Wang et al. 2012). We used
536 the package BAYPASS version 2.1 (Gautier 2015), which provides a re-implementation of the
537 Bayesian hierarchical model, and explicitly accounts for the covariance structure among the
538 population allele frequencies that originate from the shared history of the populations through the
539 estimation of the population covariance matrix. This renders the identification of SNPs subjected
540 to selection less sensitive to the confounding effect of population demography (Günther and
541 Coop 2013). Population structure was estimated by choosing a random and unlinked set of
542 10,000 SNPs and running BAYPASS under the core model (*i.e.* no covariates). Then the Bayes
543 factors (BF) were calculated running BAYPASS under the STD covariate model to evaluate
544 association of SNPs with environmental variables (*i.e.* adjusting for population structure). For
545 each SNP, the Bayes factor (denoted BF_{is} as in Gautier 2015) was presented in decibian units
546 (db) via the transformation $10 \log_{10}$ (BF). BF_{is} relies on the importance sampling algorithm
547 proposed by Coop et al., 2010 and uses MCMC samples obtained under the core model. To
548 produce a narrower set of outlier loci, we followed the popular Jeffreys' rule (Jeffreys 1961) that
549 identified outlier loci with $BF \geq 10$. As genome scan methods that correct for population
550 structure can remove some potential signals of local adaption when there is covariation between
551 the demographic history of the species and the environmental variables or phenotypic traits of
552 interest, we also calculated Spearman's rank correlation (ρ, uncorrected GEA) between
553 population allele frequencies for each SNP and each environment variable.

554 GWAS analysis was performed 86, 30 and 69 developmental and morphologic traits in *H.*
555 *annuus, H. argophyllus* and *H. petiolaris,* respectively (Supplementary table 1). 29 variables
556 were measured in all three focal species, and 39 were measured only in *H. annuus* and in *H.*
557 *petiolaris* subspecies (Supplementary table 1). Seed and flower traits could not be collected for
558 *H. argophyllus*, since most plants of this species flowered very late in our common garden, and
559 failed to form fully developed inflorescences and set seeds before temperatures became too low
560 for their survival. Population structure was controlled for in GWAS by including the first three
561 principal components as covariates, as well as an identity-by-state (IBS) kinship matrix
562 calculated by EMMAX (Kang et al. 2010). We ran each trait GWAS using EMMAX
563 (v07Mar2010), as well as the EMMAX module in EasyGWAS (Grimm et al. 2017). For every
564 SNP/peak above the Bonferroni significance threshold, candidate genes were selected within a
565 100 Kb interval centered in the SNP with the lowest p-value, or within the boundaries of the
566 GWAS peak, whichever was larger. All variants used for association were initially filtered for
567 VQSR 90% tranche, and then further filtered to only include bi-allelic SNPs genotyped in ≥ 90%
568 of samples and with a minor allele frequency ≥ 3%.

569 **Identification of top-candidate windows.** We calculated the bottom 0.05 quantiles for the *p*-
570 values from association tests, Spearman's rank correlation (uncorrected GEA) and GWAS
571 (corrected and uncorrected), yielding two 5% cutoffs. For each environmental and phenotypic
572 variable, we identified all outlier SNPs as those that fell below the respective 5% cutoff. For
573 BayPass, we considered SNPs with Bayes factor ≥ 10 as outlier SNPs. For each 5 kb window
574 that we defined across the whole genome, we counted the number of outlier SNPs (a) and the
575 total number of SNPs (n). To identify top-candidate windows for each variable, we compared the
576 number of outlier SNPs per each 5 kb window to the 0.9999 quantile of the binomial expectation
577 where the expected frequency of outlier SNPs per window is calculated as: $\rho = \sum a_i/n_i$
578 (summation over all 5 kp windows), calculating ρ independently for each environmental and
579 phenotype variable and excluding windows with 0 outliers from the calculation of ρ (as per
580 Yeaman et al. 2016). We also calculated a top candidate index using the same approach to
581 categorize outliers, obtaining a *p*-value for a binomial test for the number of SNPs per window
582 given an expected proportion of outliers (ρ; this *p*-value is not exact due to non-independence of
583 SNPs so we refer to this as an index).

584 Identifying outlier SNPs detected by genome scans from genome-wide distribution without
585 accounting for local recombination rate variation can promote false positive signals in
586 recombination cold spots (i.e., low recombination regions) and be overly conservative in
587 recombination hot spots (i.e., high recombination regions) (Booker et al. 2020). Therefore, to
588 account for local recombination rate variation, all genomic windows were binned by their
589 estimated recombination rates into 5 equally sized bins (bin1: 0-20% quantile, bin2: 20%-40%
590 quantile, bin3: 40%-60% quantile, bin4: 60%-80% quantile, bin5: 80%-100% quantile). For each
591 recombination bin, we estimated expected frequency of SNPs per window (ρ) and calculated cut-
592 off separately. Windows falling above the threshold were identified as top candidate windows.

593 **Genome-wide survey of repeatability (null-W test).** To explore repeatable genomic signatures
594 of adaptation for each of the six pairwise contrasts among the 4 taxa (Figure 1), we used the
595 method developed by Yeaman et al. (2016) with some modifications. A common approach is to
596 identify candidates for adaptation independently in each species and then examine the overlap
597 between these lists, however this approach is quite stringent and may miss many interesting
598 signals. The null-W test is more sensitive, as it takes the list of top candidates from one species
599 and tests whether they tend to show more extreme signatures of association than expected by
600 chance. The null-W test is especially favorable when LD increased divergence of SNPs in tight
601 linkage with casual SNPs but did not raise the test values enough for a window to be classified as
602 an outlier according to the binomial test. For each top candidate window that we identified for
603 each focal species in a pair, we refer to the same window in the other species as "top candidate
604 ortholog". The null distribution for each focal species and variable was constructed by randomly
605 sampling 10,000 background SNPs from non-top candidate ortholog windows. For each non-top-
606 candidate window, we then estimated the test statistic (W) for the Wilcoxon-signed rank test vs.
607 the 10,000 background SNPs. This resulted in a null distribution representing the differences
608 between the 10,000 background SNPs and the non-top-candidate ortholog windows. These were
609 then standardized to Z-scores using the method in Whitlock and Schluter (2020):

610 $$Z = \frac{2W - n1n2}{\sqrt{n1n2(n1+n2+1)/3}} \qquad \text{(Equation 2)}$$

611

612 where n1 and n2 are the sample sizes being compared. In order to control for heterogeneity in
613 recombination rate and its possible effects on the null distribution, we estimated null distribution

614 for each recombination bin separately (5 in total, see above). We then compared the p-values and
615 bayes factors (BFs) for each focal top-candidate widow to the 10,000 background SNPs,
616 calculating the W statistics and converting into a Z-score. Empirical P-values were then
617 calculated by comparing the Z-score for each top-candidate window to the null distribution.
618 When individual windows had values of W that exceeded the bounds of the null distribution,
619 their empirical *p*-value was set to the reciprocal of the number of genes in the null distribution.
620 For each species pair, we refer to the windows identified as significant by this test as "Windows
621 of Repeated Association" or WRAs.

622

623 **Linkage disequilibrium and detection of clusters of repeated association.** Linkage
624 disequilibrium among adjacent genomic windows can result in statistical non-independence and
625 similar GEA/GWAS signatures across many windows. To identify the most significant WRAs
626 and group neighbouring windows with similar signatures of repeatability into a single "Cluster of
627 Repeated Association" (CRA), we used the following approach in each pairwise contrast, and for
628 each environmental variable and phenotype: for each variable, empirical *p*-values for all WRAs
629 were converted to *q*-values to adjust for False Discovery, then beginning with the first significant
630 WRA along the chromosome (i.e. with $q < 0.05$), we compared it to the next closest significant
631 WRA by calculating the squared Pearson correlation coefficient (r^2) on the allele frequencies
632 across all pairs of SNPs, and compared this estimate to a null distribution. To construct the null
633 distribution, we generated a distribution of LD measurements between 10,000 randomly chosen
634 windows with the same physical distance as between two significant WRAs (excluding all
635 WRAs from the null distribution). If the r^2 between the two neighboring significant WRAs was
636 greater than the 95th percentile of the null distribution, we clustered these two windows together.
637 This process was repeated successively with the next closest neighboring significant WRA,
638 walking out along the chromosome until one of two stopping criteria was reached: 1) the LD
639 between the last two windows did not exceed the 95 percent of the tail distribution or 2) the
640 distance between the initial window and the current window next to it was larger than 1 cM,
641 based on the linkage map from Todesco et al. (2020). When the first round of clustering stopped
642 due to either of these two criteria, all the clustered windows were removed from the dataset and

643 the process started with the second smallest empirical p-value. By doing this way, each
644 significant WRA will only appear in a single CRA.
645
646 **Estimating an index of shared standing variation.** As genotype calling was conducted
647 separately for each species (due to computational concerns), we estimated the amount of shared
648 standing variation based on counts of shared vs. non-shared SNPs. If two species are evolving
649 independently, the number of shared SNPs should follow a hypergeometric distribution, so we
650 used an approach similar to the C-scores (Yeaman et al. 2018) to calculate the difference
651 between the observed number of shared SNPs and the expectation, scaled by the standard
652 deviation of the hypergeometric. Because of noise and a relatively small number of SNPs per
653 window, we applied this approach on a sliding window basis, including the 5 flanking windows
654 upstream and downstream of each focal window the calculation of its index of shared standing
655 variation.

656 **Correspondence between regions of repeated association and chromosomal**
657 **rearrangements.** To assess the extent of overlap between regions of the genome with repeated
658 signatures of association and previously identified low-recombination haploblocks, we used two
659 approaches. Firstly, for each pairwise species contrast and variable, we constructed a
660 contingency table for the number of top candidates that were significant WRAs vs. not-
661 significant WRAs (by the null-W test), and that did vs. did not fall within a haploblock. We
662 calculated the Pearson's χ^2 statistic on this table, and then permuted the location of haploblocks
663 throughout the genome to construct a null distribution of χ^2 statistics, and calculated the p-value
664 as the proportion of the null that exceeded the observed χ^2 statistic (to account for non-
665 independence of nearby WRAs). Secondly, we compared observations of the length and number
666 of overlapping regions to expectations based on a randomization approach. For each pair of
667 species, we kept the position of each CRA constant and randomized the position of haploblocks
668 10,000 times to build a null distribution. By keeping the position of the CRAs constant, we
669 maintained the architecture of adaptation independent from chromosomal rearrangements. We
670 assessed significance by testing whether the observed overlaps between CRAs and haploblocks
671 were more extreme than the 95th percentile of the tail of null distribution. Details about
672 identifying chromosomal rearrangements can be found in Todesco et al. (2020).

673 **Identifying repeated signatures of association across all taxa**. As a complement to the
674 pairwise analysis, we used PicMin (Booker et al. 2022a) to identify windows of the genome with
675 strong signatures of association in multiple (sub-) species. For each environmental variable,
676 association signatures for each window are ranked genome-wide and PicMin identifies windows
677 with extreme ranks in multiple species. We ran the analysis once with each of the two 3-way
678 comparisons involving one *petiolaris* subspecies (i.e. *H. annuus, H. argophyllus,* and either *H.*
679 *pet. petiolaris* or *H. pet. fallax*) to control for repeatability arising from similar patterns in the
680 two *petiolaris* subspecies (due to high introgression/shared standing variation).

681 **Evaluating genotypic redundancy using C-scores.** Genome-wide quantification of the
682 repeatability of association statistics provides insights into the amount of genotypic redundancy
683 underlying a trait or environmental adaptation, and can be assessed using the C-score approach
684 (Yeaman et al. 2018). Briefly, for a given trait or environment, the set of association test scores
685 within each species is classified into "associated" or "non-associated" using the binomial top
686 candidate approach. For a given pair of species (i = 1, 2), the observed number of associated
687 windows in each species (a_1, a_2) can be compared to the number of windows that are associated
688 in both species (a_b) and the total number of windows being analysed (a_x). Under a null
689 hypothesis where all windows in the genome have equal potential to be involved in adaptation
690 (i.e. associated with the trait or environment), the expected number of windows associated in
691 both species will be described by a hypergeometric distribution, with the expectation $\overline{a_b} =$
692 $a_1 a_2 / a_x$. The difference between the observed and expected amount of overlap in association
693 scores can be quantified as a C-score by scaling the difference by the standard deviation of the
694 hypergeometric (i.e. a C-score of 2 means that the observed amount of overlap is two standard
695 deviations above the expectation under randomness).
696 We assess the C-scores for each phenotype and environment trait by classifying the top
697 0.5% of all 5 kb windows within each species as "associated" (a_i; based on the binomial top
698 candidate index), and begin by calculating the C-score obtained when a_x is set to the union of a_i
699 across all four focal species/sub-species (i.e. only those windows associated in at least one
700 species are included in a_x, a number much lower than the total number of windows in the
701 genome). This yields a negative C-score, as a random draw from such a small number of
702 windows tends to yield many more overlapping associations by chance than the observation.

703 When the C-score = 0, it means that the observed overlap between the pair of taxa being
704 considered is consistent with a random draw of their respective "associated" windows from an
705 overall pool of a_x windows. Thus, by adding rows to the matrix with "non-associated" scores for
706 all 4 species/sub-species until finding the matrix that yields C-score = 0, we can estimate the
707 effective number of loci that contributed to variation for the trait or environment being
708 considered (L_{eff}), under the assumption that all such $a_x = L_{eff}$ windows had an equal chance of
709 contributing to the associations.

710 To run the C-score analysis on LD-clustered windows, we ran the following algorithm for
711 each trait/environmental variable: for each species, we identified all CRAs that also had a top
712 candidate index in top 0.5%. In most cases, a large cluster with associated windows in one
713 species corresponds to either no clusters or a small cluster in another species. To harmonize
714 cluster boundaries across species, we bin any overlapping clusters together to their maximum
715 extent, and take the average top candidate index for each cluster in each species as either: (a) the
716 mean across all windows that were "associated" in that species or (b) the average across all
717 windows associated in any species, if no windows were associated in that species. This yields a
718 matrix that can be submitted to the hypergeometric C-score analysis.

719

720 **Data availability**

721 All scripts used for analysis and figures will be deposited in a Dryad archive along data files and
722 results. Raw sequence data are deposited in the Sequence Read Archive (SRA) under BioProject
723 accessions PRJNA532579, PRJNA398560, and PRJNA564337, as described in Todesco et al.
724 (2020). During review, the materials for the Dryad archive are available here:
725 https://www.dropbox.com/sh/cwa34fu2o7tn6dm/AADK56Bnmx8IhQxVK70Evbgra?dl=0

726

727 **Acknowledgements**:

728 The authors would like to thank the Yeaman and Peichel labs for comments. Computational
729 support was provided by the Digital Resources Alliance of Canada, and funding was provided by

730 Genome Canada and Genome BC (LSARP2014-223SUN) and the International Consortium for
731 Sunflower Genomic Resources. SY was funded by Alberta Innovates and NSERC Discovery.
732 GLO was funded by a Banding Postdoctoral Fellowship.

733

734

735 **References:**

736 Acharya BR, Raina S, Maqbool SB, Jagadeeswaran G, Mosher SL, Appel HM, Schultz JC,
737 Klessig DF, Raina R. 2007. Overexpression of CRK13, an Arabidopsis cysteine-rich
738 receptor-like kinase, results in enhanced resistance to Pseudomonas syringae:
739 Overexpression of CRK13 induces pathogen defense. *The Plant Journal* 50:488–499.

740 Auge GA, Penfield S, Donohue K. 2019. Pleiotropy in developmental regulation by flowering-
741 pathway genes: is it an evolutionary constraint? *New Phytol* 224:55–70.

742 Aukerman MJ, Sakai H. 2003. Regulation of Flowering Time and Floral Organ Identity by a
743 MicroRNA and Its *APETALA2* -Like Target Genes. *Plant Cell* 15:2730–2741.

744 Balasubramanian S, Sureshkumar S, Agrawal M, Michael TP, Wessinger C, Maloof JN, Clark R,
745 Warthmann N, Chory J, Weigel D. 2006. The PHYTOCHROME C photoreceptor gene
746 mediates natural variation in flowering and growth responses of Arabidopsis thaliana. *Nat*
747 *Genet* 38:711–715.

748 Barghi N, Hermisson J, Schlötterer C. 2020. Polygenic adaptation: a unifying framework to
749 understand positive selection. *Nat Rev Genet* 21:769–781.

750 Barton NH, Etheridge AM, Véber A. 2017. The infinitesimal model: Definition, derivation, and
751 implications. *Theoretical Population Biology* 118:50–73.

752 Bhatia N, Bozorg B, Larsson A, Ohno C, Jönsson H, Heisler MG. 2016. Auxin Acts through
753 MONOPTEROS to Regulate Plant Cell Polarity and Pattern Phyllotaxis. *Current Biology*
754 26:3202–3208.

755 Blackman BK, Scascitelli M, Kane NC, Luton HH, Rasmussen DA, Bye RA, Lentz DL,
756 Rieseberg LH. 2011. Sunflower domestication alleles support single domestication center
757 in eastern North America. *Proc. Natl. Acad. Sci. U.S.A.* 108:14360–14365.

758 Bohutínská M, Vlček J, Yair S, Laenen B, Konečná V, Fracassetti M, Slotte T, Kolář F. 2021.
759 Genomic basis of parallel adaptation varies with divergence in *Arabidopsis* and its
760 relatives. *Proc. Natl. Acad. Sci. U.S.A.* 118:e2022713118.

Booker TR, Yeaman S, Whitlock MC. 2020. Variation in recombination rate affects detection of outliers in genome scans under neutrality. *Mol Ecol* 29:4274–4279.

Booker TR, Yeaman S, Whitlock MC. 2023a. Using genome scans to identify genes used repeatedly for adaptation. *Evolution* 77:801-811.

Booker TR, Yeaman S, Whitlock MC. 2023b. The WZA: A window-based method for characterizing genotype-environment association. *Mol Ecol Res* (in press).

Bürger R, Akerman A. 2011. The effects of linkage and gene flow on local adaptation: A two-locus continent–island model. *Theoretical Population Biology* 80:272–288.

Chen A, Li C, Hu W, Lau MY, Lin H, Rockwell NC, Martin SS, Jernstedt JA, Lagarias JC, Dubcovsky J. 2014. PHYTOCHROME C plays a major role in the acceleration of wheat flowering under long-day photoperiod. *Proc. Natl. Acad. Sci. U.S.A.* 111:10037–10044.

Cheval C, Perez M, Leba LJ, Ranty B, Perochon A, Reichelt M, Mithöfer A, Robe E, Mazars C, Galaud JP, et al. 2017. PRR2, a pseudo-response regulator, promotes salicylic acid and camalexin accumulation during plant immunity. *Sci Rep* 7:6979.

DeRaad DA, Cobos ME, Alkishe A, Ashraf U, Ahadji-Dabla KM, Nuñez-Penichet C, Peterson AT. 2021. Genome-environment association methods comparison supports omnigenic adaptation to ecological niche in malaria vector mosquitoes. *Molecular Ecology* 30:6468–6485.

Dong MA, Farré EM, Thomashow MF. 2011. CIRCADIAN CLOCK-ASSOCIATED 1 and LATE ELONGATED HYPOCOTYL regulate expression of the C-REPEAT BINDING FACTOR (CBF) pathway in *Arabidopsis*. *Proc. Natl. Acad. Sci. U.S.A.* 108:7241–7246.

Gautier M. 2015. Genome-Wide Scan for Adaptive Divergence and Association with Population-Specific Covariates. *Genetics* 201:1555–1579.

Grimm DG, Roqueiro D, Salomé PA, Kleeberger S, Greshake B, Zhu W, Liu C, Lippert C, Stegle O, Schölkopf B, et al. 2017. easyGWAS: A Cloud-Based Platform for Comparing the Results of Genome-Wide Association Studies. *Plant Cell* 29:5–19.

Günther T, Coop G. 2013. Robust Identification of Local Adaptation from Allele Frequencies. *Genetics* 195:205–220.

Hager ER, Harringmeyer OS, Wooldridge TB, Theingi S, Gable JT, McFadden S, Neugeboren B, Turner KM, Jensen JD, Hoekstra HE. 2022. A chromosomal inversion contributes to divergence in multiple traits between deer mouse ecotypes. *Science* 377:399–405.

Heiser C, Smith D, Clevenger S, Martin W. 1969. The North American sunflowers (Helianthus). *Memoirs of the Torrey Botanical Club* 22:1–218.

Heiser, CB. 1951. Hybridization in the Annual Sunflowers: Helianthus annuus x H. argophyllus. *The American Naturalist* 85:65–72.

797 Hoban S, Kelley JL, Lotterhos KE, Antolin MF, Bradburd G, Lowry DB, Poss ML, Reed LK,
798 Storfer A, Whitlock MC. 2016. Finding the Genomic Basis of Local Adaptation: Pitfalls,
799 Practical Solutions, and Future Directions. *The American Naturalist* 188:379–397.

800 Izawa T. 2007. Adaptation of flowering-time by natural and artificial selection in Arabidopsis
801 and rice. *Journal of Experimental Botany* 58:3091–3097.

802 Jeffreys H. 1961. Theory of probability. 3rd ed. New York, NY: Oxford University Press

803 Kang HM, Sul JH, Service SK, Zaitlen NA, Kong S, Freimer NB, Sabatti C, Eskin E. 2010.
804 Variance component model to account for sample structure in genome-wide association
805 studies. *Nat Genet* 42:348–354.

806 Keuskamp DH, Pollmann S, Voesenek LACJ, Peeters AJM, Pierik R. 2010. Auxin transport
807 through PIN-FORMED 3 (PIN3) controls shade avoidance and fitness during
808 competition. *Proc. Natl. Acad. Sci. U.S.A.* 107:22740–22744.

809 Kirkpatrick M, Barton N. 2006. Chromosome Inversions, Local Adaptation and Speciation.
810 *Genetics* 173:419–434.

811 Láruson ÁJ, Yeaman S, Lotterhos KE. 2020. The Importance of Genetic Redundancy in
812 Evolution. *Trends in Ecology & Evolution* 35:809–822.

813 Lee C-R, Wang B, Mojica JP, Mandáková T, Prasad KVSK, Goicoechea JL, Perera N, Hellsten
814 U, Hundley HN, Johnson J, et al. 2017. Young inversion with multiple linked QTLs
815 under selection in a hybrid zone. *Nat Ecol Evol* 1:0119.

816 Liu Z, Jia Y, Ding Y, Shi Y, Li Z, Guo Y, Gong Z, Yang S. 2017. Plasma Membrane CRPK1-
817 Mediated Phosphorylation of 14-3-3 Proteins Induces Their Nuclear Import to Fine-Tune
818 CBF Signaling during Cold Response. *Molecular Cell* 66:117-128.e5.

819 Lotterhos KE, Whitlock MC. 2014. Evaluation of demographic history and neutral
820 parameterization on the performance of F_{ST} outlier tests. *Mol Ecol* 23:2178–2192.

821 MacPherson A, Nuismer SL. 2017. The probability of parallel genetic evolution from standing
822 genetic variation. *J. Evol. Biol.* 30:326–337.

823 Manceau M, Domingues VS, Linnen CR, Rosenblum EB, Hoekstra HE. 2010. Convergence in
824 pigmentation at multiple levels: mutations, genes and function. *Phil. Trans. R. Soc. B*
825 365:2439–2450.

826 Mizoguchi T, Wheatley K, Hanzawa Y, Wright L, Mizoguchi M, Song HR, Carré IA, Coupland
827 G. 2002. LHY and CCA1 are partially redundant genes required to maintain circadian
828 rhythms in Arabidopsis. *Dev Cell* 2:629–641.

829 Moyers BT, Rieseberg LH. 2016. Remarkable life history polymorphism may be evolving under
830 divergent selection in the silverleaf sunflower. *Mol Ecol* 25:3817–3830.

831 Ostevik KL, Andrew RL, Otto SP, Rieseberg LH. 2016. Multiple reproductive barriers separate
832 recently diverged sunflower ecotypes: reproductive barriers between sunflower ecotypes.
833 *Evolution* 70:2322–2335.

834 Para A, Farré EM, Imaizumi T, Pruneda-Paz JL, Harmon FG, Kay SA. 2007. PRR3 Is a vascular
835 regulator of TOC1 stability in the Arabidopsis circadian clock. *Plant Cell* 19:3462–3473.

836 Pekker I, Alvarez JP, Eshed Y. 2005. Auxin response factors mediate Arabidopsis organ
837 asymmetry via modulation of KANADI activity. *Plant Cell* 17:2899–2910.

838 Rosenblum EB, Parent CE, Brandt EE. 2014. The Molecular Basis of Phenotypic Convergence.
839 *Annu. Rev. Ecol. Evol. Syst.* 45:203–226.

840 Sambatti JBM, Strasburg JL, Ortiz-Barrientos D, Baack EJ, Rieseberg LH. 2012. Reconciling
841 extremely strong barriers with high levels of gene exchange in annual sunflowers: gene
842 flow across a strong reproductive barrier. *Evolution* 66:1459–1473.

843 Schaal SM, Haller BC, Lotterhos KE. 2022. Inversion invasions: when the genetic basis of local
844 adaptation is concentrated within inversions in the face of gene flow. *Phil. Trans. R. Soc.*
845 *B* 377:20210200.

846 Strasburg JL, Rieseberg LH. 2008. Molecular demographic history of the annual sunflowers
847 *helianthus annuus* and *h. Petiolaris* -large effective population sizes and rates of long-
848 term gene flow. *Evolution* 62:1936–1950.

849 Takano M, Inagaki N, Xie X, Yuzurihara N, Hihara F, Ishizuka T, Yano M, Nishimura M,
850 Miyao A, Hirochika H, et al. 2005. Distinct and Cooperative Functions of Phytochromes
851 A, B, and C in the Control of Deetiolation and Flowering in Rice. *The Plant Cell*
852 17:3311–3325.

853 Tittes S, Lorant A, McGinty S, Doebley JF, Holland JB, Sánchez-González J de J, Seetharam A,
854 Tenaillon M, Ross-Ibarra J. 2021. Not so local: the population genetics of convergent
855 adaptation in maize and teosinte. Evolutionary Biology Available from:
856 http://biorxiv.org/lookup/doi/10.1101/2021.09.09.459637

857 Todesco M, Owens GL, Bercovich N, Légaré J-S, Soudi S, Burge DO, Huang K, Ostevik KL,
858 Drummond EBM, Imerovski I, et al. 2020. Massive haplotypes underlie ecotypic
859 differentiation in sunflowers. *Nature* 584:602–607.

860 Visscher PM, Wray NR, Zhang Q, Sklar P, McCarthy MI, Brown MA, Yang J. 2017. 10 Years
861 of GWAS Discovery: Biology, Function, and Translation. *The American Journal of*
862 *Human Genetics* 101:5–22.

863 Wang L, Josephs EB, Lee KM, Roberts LM, Rellán-Álvarez R, Ross-Ibarra J, Hufford MB.
864 2021. Molecular Parallelism Underlies Convergent Highland Adaptation of Maize
865 Landraces.Purugganan M, editor. *Molecular Biology and Evolution* 38:3567–3580.

Wang T, Hamann A, Spittlehouse DL, Murdock TQ. 2012. ClimateWNA—High-Resolution Spatial Climate Data for Western North America. *Journal Of Applied Meteorology And Climatology* 51:14.

Wellenreuther M, Bernatchez L. 2018. Eco-Evolutionary Genomics of Chromosomal Inversions. *Trends in Ecology & Evolution* 33:427–440.

Whitlock M, Schluter D. 2020. The analysis of biological data. 3rd ed. Macmillan

Yang J, Lee SH, Goddard ME, Visscher PM. 2011. GCTA: A Tool for Genome-wide Complex Trait Analysis. *The American Journal of Human Genetics* 88:76–82.

Yeaman S. 2022. Evolution of polygenic traits under global *vs* local adaptation. *Genetics* 220:iyab134.

Yeaman S, Gerstein AC, Hodgins KA, Whitlock MC. 2018. Quantifying how constraints limit the diversity of viable routes to adaptation.Ralph PL, editor. *PLoS Genet* 14:e1007717.

Yeaman S, Hodgins KA, Lotterhos KE, Suren H, Nadeau S, Degner JC, Nurkowski KA, Smets P, Wang T, Gray LK, et al. 2016. Convergent local adaptation to climate in distantly related conifers. *Science* 353:1431–1433.

Yeaman S, Whitlock MC. 2011. The genetic architecture of adaptation under migration-selection balance: the genetic architecture of local adaptation. *Evolution* 65:1897–1911.